Vol. 4 No. 4 (2025)

Pakistan Journal of Medical & Cardiological Review

https://pakjmcr.com/index.php/1/about

Online ISSN 3007-2387

Print ISSN 3007-2379

Computational Modeling of Clinically Approved Alkylating Agents Against Epidermal and Fibroblast Growth Factor Receptors: A Step Toward Liver Cancer Therapeutics

Dr. Sharmeen Mehmood
Niazi Medical and Dental College Sargodha
Email: sharmeenmehmood3131@gmail.com

Saroush Mehmood*
Faculty of Science, The Superior University, Lahore
Email:sharmeenmehmood3131@gmail.com

Author Details

Keywords: Cell Proliferation; Carcinoma; Angiogenesis; Pharmacokinetics; Lipophilicity
.

Received on 15 Nov 2025
Accepted on 10 Dec 2025
Published on 23 Dec 2025

Corresponding E-mail & Author*:

Saroush Mehmood*
Faculty of Science, The Superior University, Lahore
Email:sharmeenmehmood3131@gmail.com

Abstract

Cancer is a leading cause of death, which occurs due to various factors like mutations, radiation, and many other factors. Still, no benefit has been established worldwide. To overcome this problem, the current study aimed to evaluate the anti-hepatocellular carcinoma and anti-hepatoblastoma potential of commonly used drugs against a specific type of cancer. The five most active alkylating agents, including melphalan (hepatocarcinoma), mitomycin C (anticancer and antibiotic), estramustine (prostate cancer), pipobroman (leukemia), and irofulven (prostate cancer), were selected for in silico molecular docking. The given agents were downloaded from PubChem with CID 460612, 5746, 259331, 4842, and 148189, respectively. The protein targets epidermal growth factor (HER2) and fibroblast growth factor were retrieved from the Protein Data Bank with PDB IDs 1N8Z and 6NVG. The target and ligands were optimized or prepared to perform virtual screening and toxicity studies. The physicochemical, lipophilicity, water solubility, pharmacokinetics, and drug likeness were analyzed. The molecular docking results showed that estramustine exhibited greater inhibition against HER2 and fibroblast growth factor, with binding energies of -7.9 and -7.7 Kcal/mol, respectively, compared to other alkylating agents. But other agents also exhibited inhibitory potential against the HER2 and fibroblast growth factor, using strong hydrogen bonding with reasonable binding energies. The computational approach reflects that the specific targeted anticancer agents attenuate the activities of the selected targets by inhibiting the major signaling pathways, such as angiogenesis and cancer cell proliferation. The finding suggested that the specifically targeted drugs could be used against hepatocarcinoma or hepatoblastoma.

Introduction

A leading cause of mortality globally, cancer imposes an immense fiscal burden on public healthcare systems (Diseases GBD and Injuries C, 2024; WHO, 2024). There

is great variation in the incidence, mortality, and cancer DALY burden in different regions and nations, with large gaps between industrialized and developing nations (Bray et al., 2024). More than 90% of cancer fatalities are due to tumor metastases, which are an imperative step in malignancy development and present a great challenge for therapeutic management in the vast majority of advanced cancer patients (Welch and Hurst, 2019). This multifaceted process involves malignant cells crossing tissue barriers and uncontrolled expansion of primary tumor foci, both of which give rise to new lesions in distant organs. Quality of life and survival in patients are irreparably damaged by this (Quintanal-Villalonga et al., 2020). The wide variation in cancer incidence rate, mortality rate, and DALY burden is due to a variety of reasons, such as ecological, environmental, demographic, cultural, and genetic effects (Collaborators GBDCRF, 2020). In 2022, 19,976,499 new cancer cases (including non-melanoma skin cancers) were diagnosed across the world, based on estimated data from GLOBOCAN 2022 (Diao et al., 2025). The optimum way to reduce infection-related cancers, such as those of the liver, cervix, stomach, and nasopharynx, is prevention of chronic infections (Han-You X, 2013). In 2022, prostate cancer (1.47 million) and lung cancer (1.57 million new cases [95% UI: 1.56–1.58]) were the two most common cancers that were diagnosed in men worldwide. Breast cancer was the most frequent cancer to be diagnosed in women in 2022 and was expected to occur in 2.30 million (2.28–2.30) cases. The next two most frequent cancers to be diagnosed in women were lung cancer at 0.91 million (0.90–0.91 million) and cervical cancer at 0.66 million (0.66–0.67). The leading causes of cancer deaths among women and men were breast cancer (0.67 million [0.66–0.67]) and lung cancer (1.23 million [1.22–1.24]), respectively (Filho AM et al., 2025).

The liver is a multifunctional organ involved in regulating immunological response, protein synthesis, metabolism, and detoxification (Santos et al., 2024). Hepatocytes are the predominant parenchymal cells of the liver and are largely responsible for mediating these functions. Hepatic stellate cells (HSCs), cholangiocytes, Kupffer cells (KCs), liver sinusoidal endothelial cells (LSECs), and other immune cell types that maintain liver homeostasis contribute to these (Schulze et al., 2019). LSECs with unique fenestrations border the liver sinusoids, thereby providing extreme interactions among hepatocytes and sinusoids. Several instances of genetic alterations of Wnt signaling in human HCC have been reported. Mutations of the β-catenin gene (CTNNB-1) that result in the inhibition of β-catenin degradation and its nuclear translocation are found in 8–30% of patients with HCC (Rebouissou et al., 2016; Laurent–Puig et al., 2001).

Due to its very high mortality rate, hepatocellular carcinoma (HCC) is the most common type of primary liver cancer and a significant global health issue. Hepatitis B and hepatitis C virus infection, alcohol consumption, and metabolic conditions such as metabolic dysfunction-associated steatotic liver disease (MASLD) are the primary etiologies of chronic liver diseases, which have an intimate association with the epidemiology of HCC (Singh et al., 2025). Wnt signaling is pathologically enhanced in human HCC tissues, as reported by integrated multi-omics studies (Sun et al., 2024). Interestingly, in human HCC cells, Wnt-3a and Fzd-7 cooperate to stimulate β-catenin-dependent signaling, with the ability to enhance tumor growth and cell migration (Kim et al., 2008). Interestingly, HCC cannot be triggered solely by β-catenin protein activation and hepatocyte-specific overexpression (Cadoret et al., 2001). Conversely, β-catenin activation with pathogenic signals could initiate and accelerate the development of HCC in mice (Nejak-Bowen et al., 2010). But these data are contradicted by the fact that the liver of Ctnnb-1 conditional deletion develops 7-fold greater tumor cell frequency than that of the wild type, implying that the absence of β-catenin favors carcinogen-induced carcinogenesis.

The heterogeneity and complexity of cancer make it challenging to identify new drugs and therapeutic regimens with sustained effects in most patients despite the spectacular progress of the past decade. Development of targeted treatments compatible with the genetic and molecular characteristics of cancer will be a prerequisite for future progress in the treatment of cancer (Arafeh et al., 2025). We selected the most commonly employed alkylating agents based on earlier studies, most of which are employed to treat cancers other than HCC. A catalog of enzymes that play a role in the generation of cancer via overexpression. These enzymes are telomerase, lipid metabolic enzymes, tyrosine kinases, serine/threonine kinases, matrix metalloproteinases (MMPs), cysteine proteases, DNA polymerase, DNA helicases, glycolytic enzymes, and enzymes that modify histones. Cell growth and proliferation are mediated by the human epidermal growth factor receptor 2 (HER2). HER2 functioned by suppressing SMAD3 and enhancing β-catenin. HER2 overexpression however inhibits angiogenesis, cell cycle, and apoptosis (Shi et al., 2019).

The past 30 years have witnessed the application of many pharmacological and therapy groups. Plant metabolites, synthetic drugs like alkylating agents, platinum drugs, hormone therapy, and chemotherapy are some of these groups. Through normalization of signal pathways, alkylating agents—the most promising anticancer agent family substantially enhance inhibition of overexpressed receptors or enzymes. Cyclophosphamide, ifosfamide, melphalan, and chlorambucil are the most frequently used alkylating agents in cancer treatment (Singh et al., 2025). The nature of cancer as a complex and heterogeneous disease makes it challenging to identify new treatments and combinations that have enduring consequences for most patients, despite the great strides in the past decade (Arafeh et al., 2025).

Based on the mode of action of alkylating agents, we selected five alkylating agents with broad application against different types of carcinomas. These alkylating agents are melphalan, mitomycin C, estramustine, irofulven, and pipobroman. Melphalan is mostly used against hepatocellular carcinoma, myeloma, ovarian carcinoma, melanoma, and amyloidosis (Anafcheh et al., 2012; Pocasap et al., 2021). The anticancer drug mitomycin C (MMC), is an anti-cancer antibiotic derived from bacteria that undergo enzymatic bio-reduction in order to exert a biological effect. MMC is converted to a very reactive bis-electrophilic intermediate that alkylates cell nucleophiles. The most desirable mode of action of MMC is alkylation of DNA, but the drug's biological activity can be affected by other mechanisms as well, such as redox cycling and inhibition of rRNA. Cellular nucleophiles are alkylated by the extremely reactive bis-electrophilic intermediate formed from MMC. While MMC's preferred mechanism of action is alkylation of DNA, other mechanisms of action, such as redox cycling and rRNA inhibition, potentially could be implicated in the drug's biological activities. Herein, we show that MMC also targets the thioredoxin reductase (TrxR) in cells. We show that MMC inhibits TrxR in vivo with cancer cell cultures and in vitro with purified enzyme (Paz et al., 2012).

The current research is designed to evaluate the anti-hepatic carcinogenic potential of specified alkylating agents commonly used against particular cancers via computational approaches.

Materials and Methods

Computational modeling nowadays is extensively used to determine the interaction of drugs or medicated herbs with the protein targets, which are commonly an enzyme responsible for inducing cancer inside the body. Various metabolic /signaling pathways involved in the process of cancer and their effects throughout the body, such pathways include cell proliferations, apoptosis, cyclic dependent pathway, Receptor

Tyrosine Kinase (RTK) Pathways (Yip and Papa (2021), and PI3K/AKT/mTOR Pathway (McCubrey et al., 2015).
National Center for Biotechnology Information (NCBI) database, Protein Data Bank (PDB), PubChem, ChemSpider, and NIST were all extensively used to retrieve the target and ligands with their pharmacological potential against various ailments, especially cancer. These databases provided 2D and 3D versions of protein targets and ligands and generated a file in different types of extensions, like SDF, mol, etc. The protein targets and ligands are optimized or prepared to perform virtual screening and toxicity studies.
The five anticancer drugs, such as melphalan, mitomycin C, estramustine, irofulven, and pipobroman, were downloaded from PubChem. The energy minimization was performed using Avogadro2 and then saved in SDF format for further analysis.
The HER2 protein target (also known as Neu, ErbB2) is a member of the epidermal growth factor receptor family of receptor tyrosine kinases known as the ErbB, whose members in humans include HER1 (EGFR, ERBB1), HER2, HER3, and HER4 (ERBB4). The origin and virulence of most cancers are associated with the aberrant activation of ErbB receptors, key players in cell growth and differentiation in developing embryos as well as adult tissues (Rubin et al., 2024). The irrelevant molecules, such as water, ligand, and metallic ions, were removed using BIOVIA Discovery Studio, and the protein target was saved in PDB format for virtual screening.

Molecular docking
The virtual screening of the target and selected ligands was performed using PYRX (Autodock 4.0.0). In the first step, uploading the target molecule and changing it to macromolecules, and saving it in PDBQT format. Next step, upload the ligand molecule using the Open Babel tab, then minimize the energy levels, and then change its format to pdbqt. Then select the grid box with the appropriate axis, and then ok the run command. After a few seconds or minutes, the virtual screening was completed, and the best pose was saved in PDB format for further visualization using BIOVIA Discovery Studio and PyMol (Akhtar et al., 2025).

Toxicity study
The toxicity study of both alkylating agents was analyzed using PROTOX online tools. In a toxicity study, we study organ toxicity, toxicity end points, nuclear receptor signaling pathways, stress response pathways, molecular initiating events, and metabolism (online protox, 2024).

ADME properties of alkylating agents
The online server was used to analyze the physicochemical, lipophilicity, water solubility, pharmacokinetics, and drug likeness of selecting alkylating agents (SwissADME, 2024).

Mode of Action Selected Ligands
The mechanism of action of three ligands, such as estramustine, mitomycin, and irofulven, was drawn using the BioRender online server.

Results
The computational modeling of the biological properties of ligands purely depends on their behavior with target proteins. The NCBI provides complete information on protein 3D structure. The protein 3D structure was retrieved from the PDB with PDB id (1N8Z) in pdb format (Fig. 1A & 1B), undergoing deactivation caused by (2S)-2-

amino-3-[4-[bis(2 chloroethyl)amino]phenyl]propanoic acid (melphalan), [(4S,6S,7R,8S)-11-amino-7-methoxy-12-methyl-10,13-dioxo-2,5-diazatetracyclo[7.4.0.0^{2,7}.0^{4,6}]trideca-1(9),11-dien-8-yl]methyl carbamate (mitomycin C), [(8R,9S,13S,14S,17S)-17-hydroxy-13-methyl-6,7,8,9,11,12,14,15,16,17-decahydrocyclopenta[a]phenanthren-3-yl] N,N-bis(2-chloroethyl)carbamate (Estrmustine), (5'R)-5'-hydroxy-1'-(hydroxymethyl)-2',5',7'-trimethylspiro[cyclopropane-1,6'-indene]-4'-one (Irofulven), and 3-bromo-1-[4-(3-bromopropanoyl)piperazin-1-yl]propan-1-one (pipobroman) (Fig. 2).

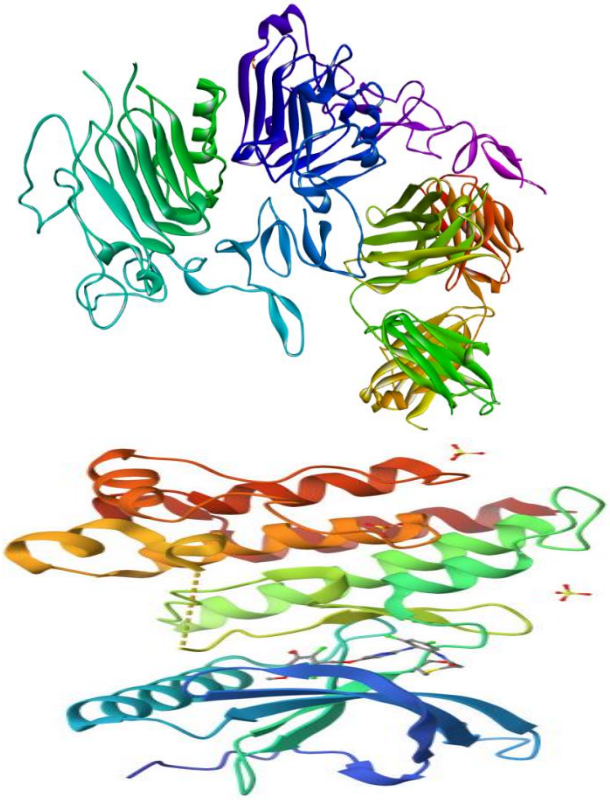

Fig. 1A: 3D structure 1N8Z from PDB

Fig. 1B: 3D structure 6NVG from PDB

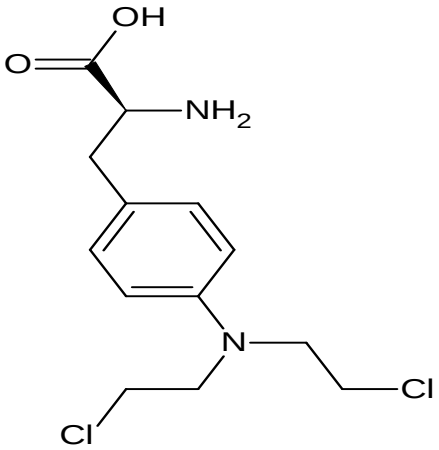

Melphalan (CID-460612)

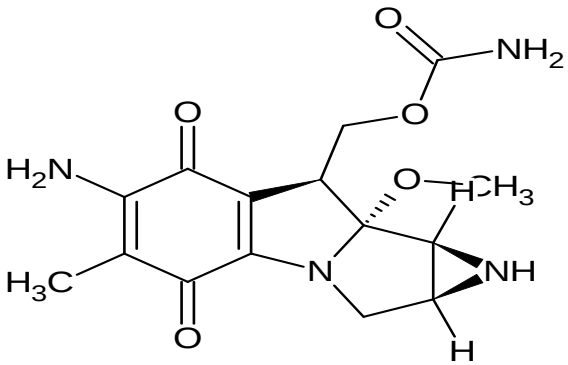

Mitomycin C (CID-5746)

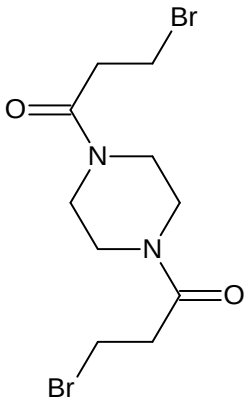

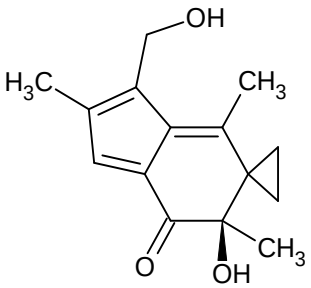

Irofulven(CID-148189)

Pipobroman (CID-4842)

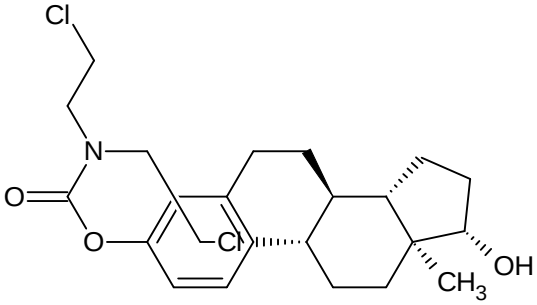

Estramustine (CID-259331)

Fig. 2: Chemical structure of selected alkylating agents drawn using ChemSketch

The results revealed that estramustine showed maximum inhibitory potential against the HER2 receptor with the binding energy of -7.9 Kcal/mol. The active site residue of HER2-B chain binds with estramustine, active site contains: Cys289, Gly 417, Ile 413, Gly 36, Gln 84, Gln 35, Thr 290, Phe 269, Gly 270, Gln 59, Tyr 281, Thr 5, Arg 412, Leu 414. Whereas, mitomycin C was the second alkylating agent which showed strong binding with the HER2 receptor, and active site, containing Cys 316, Tyr 321, His 296, Cys 293, Gln 298, Glu 299, Asn 297, Phe 349, Val 319, Arg 318. The details on binding energies and active site residues were mentioned in Table 1 & Figure 3.
Similarly, in the case of the fibroblast growth factor receptor, the strongest binding was again shown by estramustine, with a binding energy of -7.5 kcal/mol. The active site contained Leu 575, Gly 678, Phe 674, Pro 703, Leu 676, Pro 567, Gly 573, Leu 580, Thr 675, Trp 671, and Pro 682. Irofulven was the second most active inhibitory alkylating agent that binds with 6NVG with a binding energy of -7.0 kcal/mol (Table 2 & Figure 4).
The results also favour the combinatorial use of medicine against different ailments. in this study, both alkylating agents (melphalan and mitomycin) significantly inhibit both chains of HER2 receptors that take part in cell proliferation.

Table 1 Docking of selected alkylating agents against the HER2-receptor

Alkylating agents	CID	Binding Energy	Grid			Binding Interactions	Residue
			X	Y	Z		
Melphalan	460612	-6.9	0.84	86.85	129.18	H-Bonding Hydrophobic	ASN 466, GLY 442, HIS 468, LEU 443,

							LEU 414, LEU 27, THR 5, VAL 3, PHE269, PRO 278, ASN 280, TYR 279, SER 441, GLN 469,
Mitomycin C	5746	7.2				H-Bonding Hydrophobic	CYS 316, TYR 321, HIS 296, CYS 293, GLN 298, GLU 299, ASN 297, PHE 349, VAL 319, ARG 318
Estramustine	259331	-7.9				H-Bonding Hydrophobic	CYS289, GLY 417, ILE 413, GLY 36, GLN 84, GLN 35, THR 290, PHE 269, GLY 270, GLN 59, TYR 281, THR 5, ARG 412, LEU 414
Irofulven	148189	-6.8				H-Bonding Hydrophobic	THR 5, TYR 279, HIS 468, SER 441, ASN 466, THR 1, VAL 3, PRO 278, ASN 280, TYR 281, CYS 4
Pipobromin	4842	-6.0				Hydrophobic	GLY 411, ASN 280, LEU 29, TYR 281, SER 441, HIS 468, PRO 278,

							ASN 466, THR 5, LEU 414

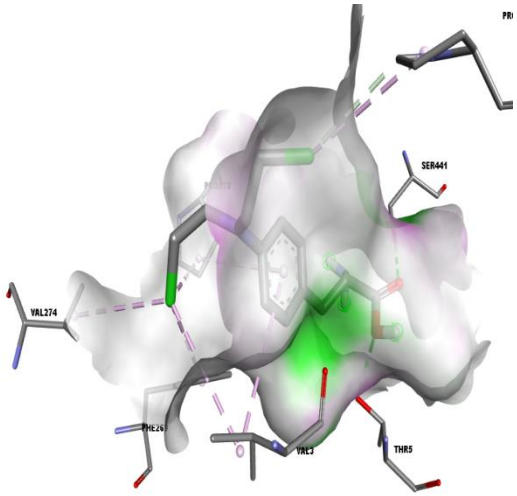

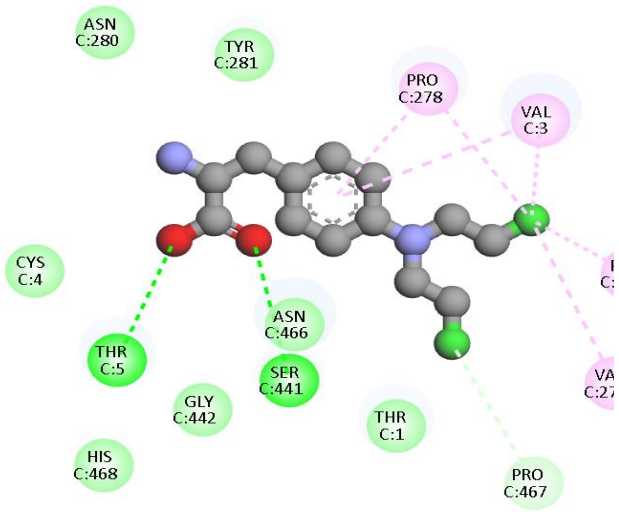

1N8Z-Melphalan (-6.9 kcal/mol)

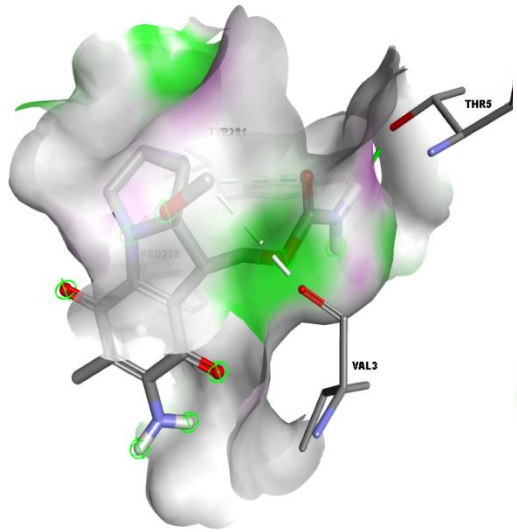

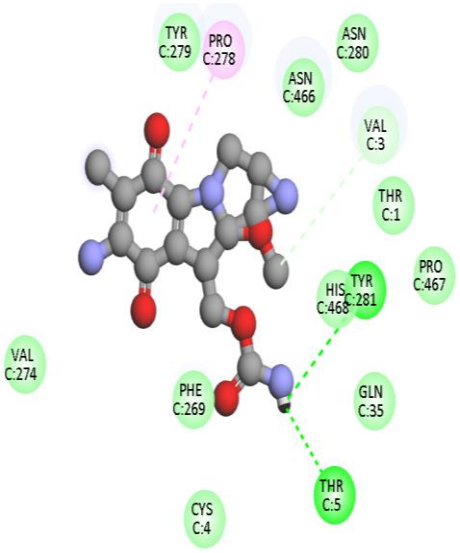

1N8Z-Mitomycin C (-7.2 kcal/mol)

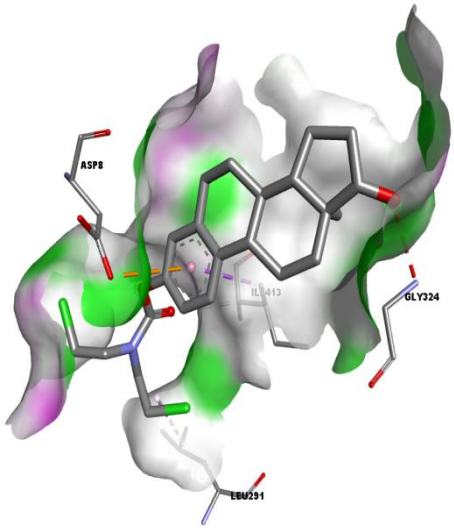

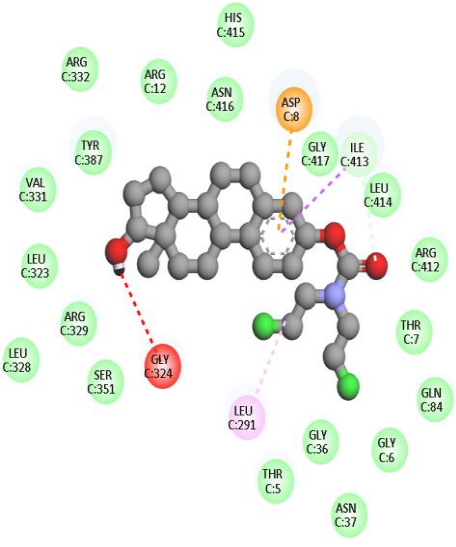

1N8Z-Estramustine (-7.9 kcal/mol)

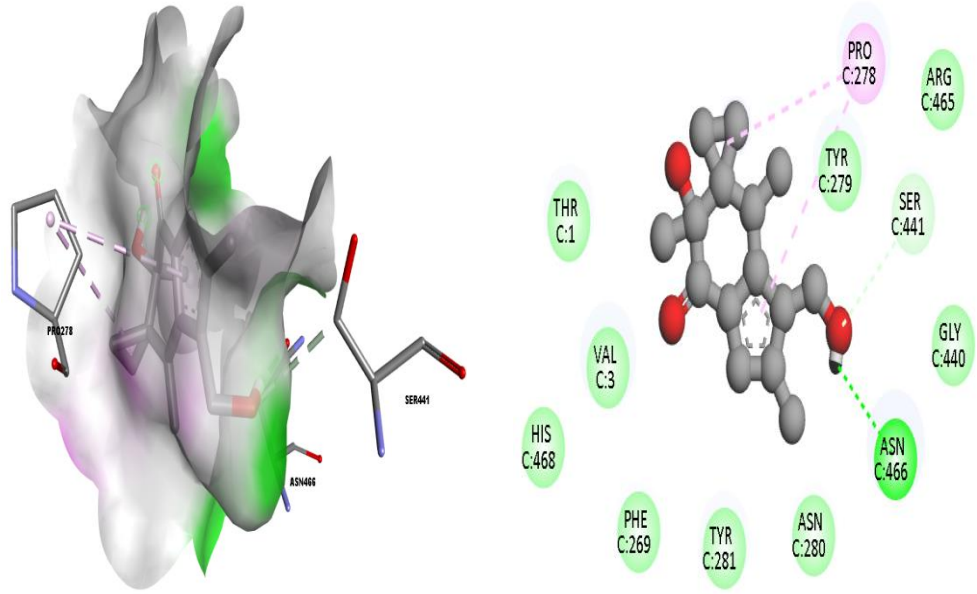

1N8Z-Irofulven (-6.8 kcal/mol)

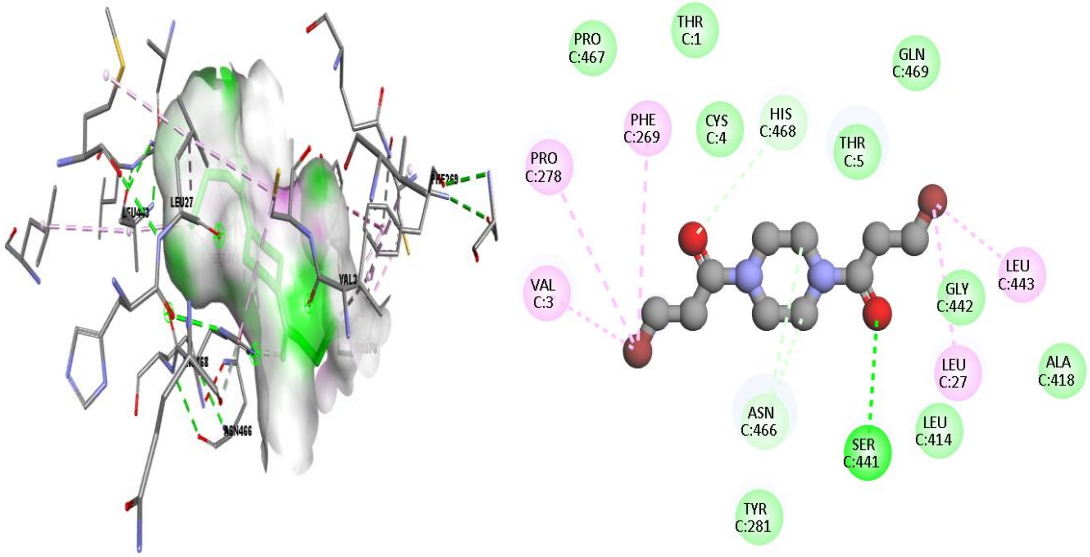

1N8Z-pipobroman (-6.0 kcal/mol)

Fig. 3: Docking of selected alkylating agents against epidermal growth factor receptor HER2

Table 2: Docking of selected alkylating agents against fibroblast growth factor (6NVG)

Alkylating agents	CID	Binding Energy	Grid			Binding Interactions	Residue
			X	Y	Z		
Melphalan	460612	-6.0	0.71	80.15	101.11	H-Bonding Hydrophobic	GLU 551, ALA 553, LEU 473, LEU 610, PHE 622, MET 524, ASP 621, VAL 550, LEU 517,

							GLU 520, LYS 503, VAL 548, CYS 552, ILE 534, VAL 481, ALA 501
Mitomycin C	5746	-6.8				H-Bonding Hydrophobic	PHE 674, PRO 567, HIS 704, PRO 703, PHE 577, LEU 575, GLY 573, LEU 676
Estramustine	259331	-7.5				H-Bonding Hydrophobic	LEU 575, GLY 678, PHE 674, PRO 703, LEU 676, PRO 567, GLY 573, LEU 580, THR 675, TRP 671, PRO 682
Irofulven	148189	-7.0				H-Bonding Hydrophobic	GLY 573, PHE 674, PRO 567, LEU 575, LEU 676, LEU 580, PRO 703, HIS 704, PHE 577, SER 576
Pipobroman	4842	-5.3				H-Bonding Hydrophobic	ALA 553, LYS 503, GLU 520, VAL 481, LEU 473, GLU 551, GLY 556, CYS 552, ALA 501, LEU 610, ASP 621, VAL 550

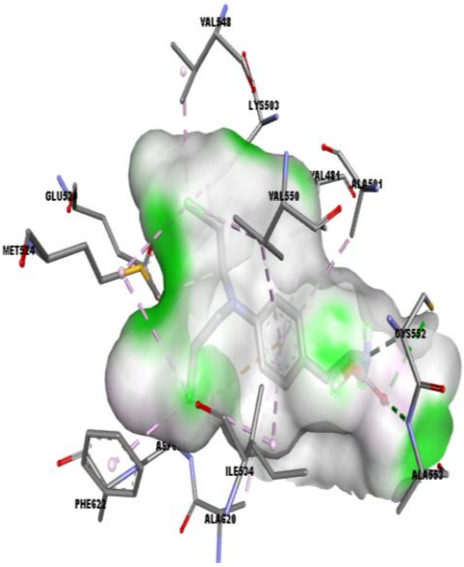

6NVG-Malphalan (-6.0 kcal/mol)

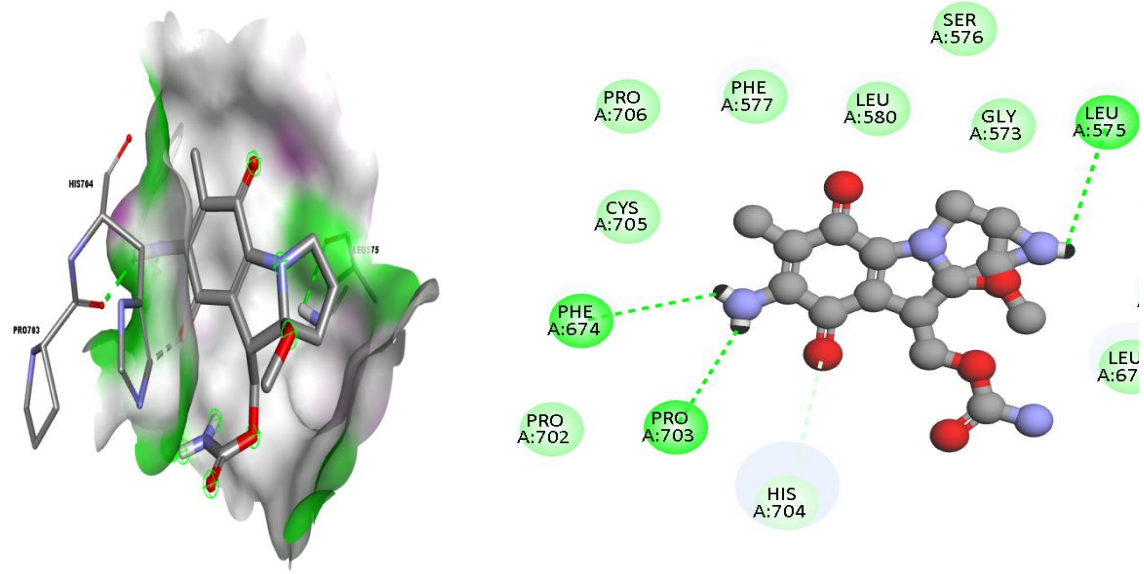

6NVG-Mitomycin (-6.8 kcal/mol)

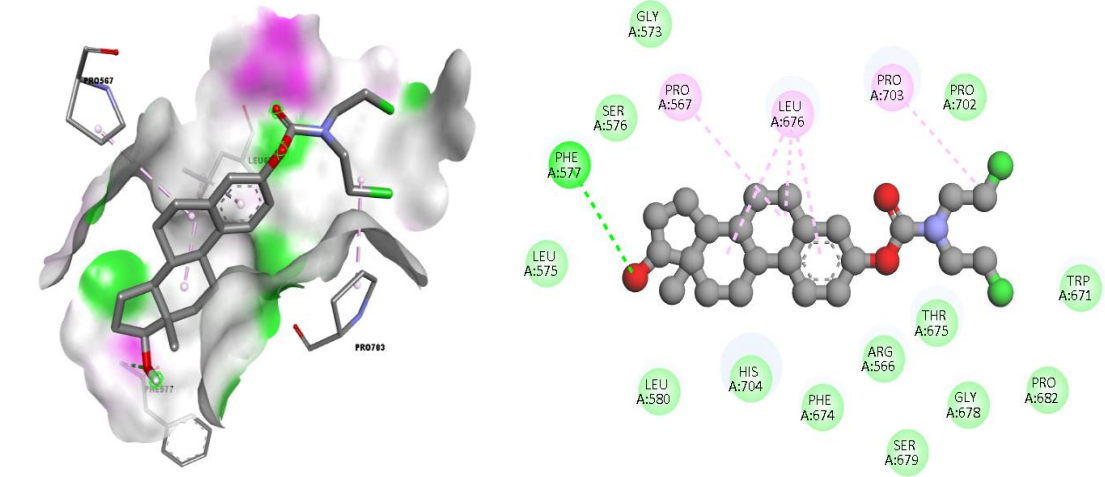

6NVG-Estramustine (-7.5 kcal/mol)

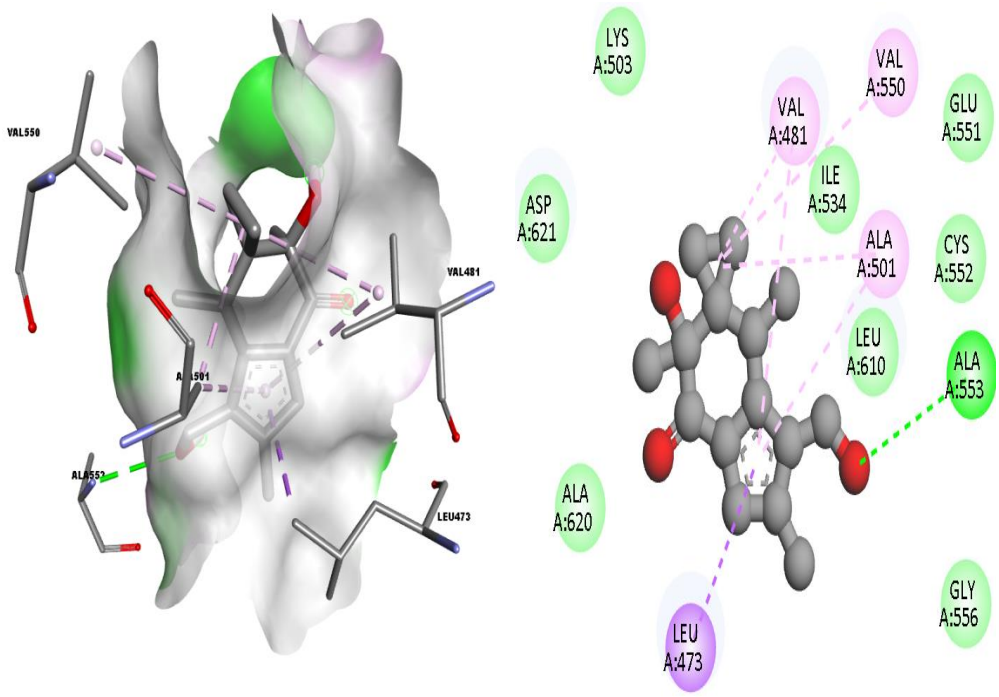

6NVG-Irofulven (-7.0 kcal/mol)

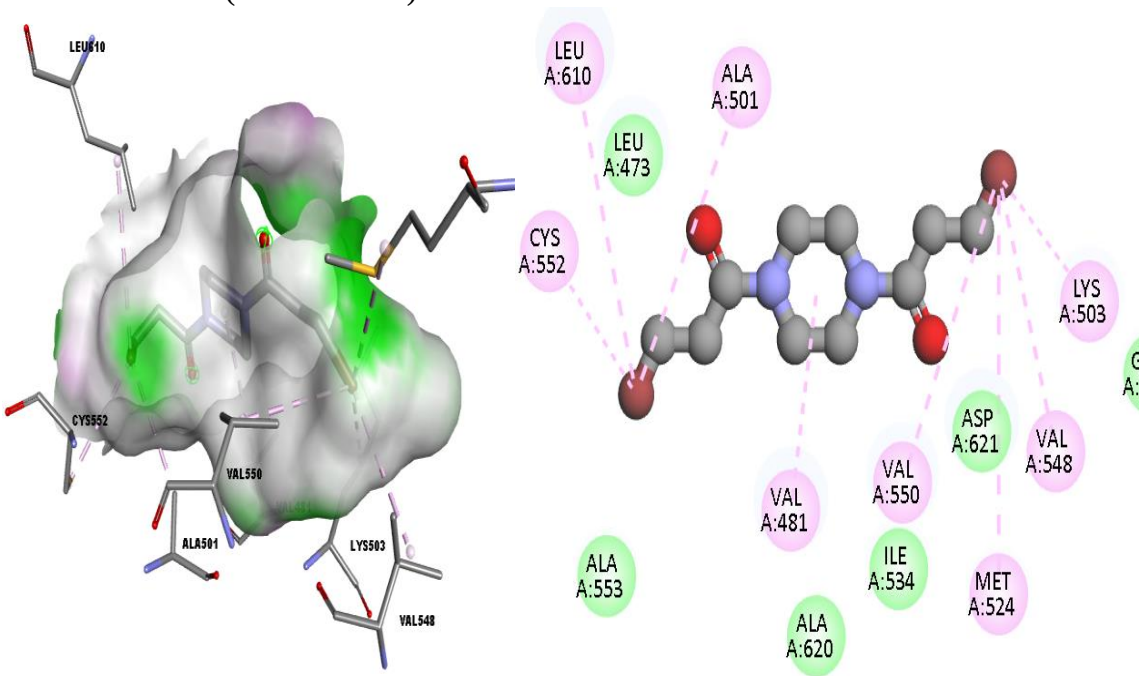

6NVG-Pipobroman (-5.6 kcal/mol)

Fig. 4: Docking of selected alkylating agents against Fibroblast growth factor receptor (6NVG)

Toxicity Evaluation

PROTOX online tools evaluated organ toxicity, end points, signaling pathways, stress response pathways, molecular processes, and metabolism. The findings showed that all selected alkylating agents, such as melphalan, mitomycin C, estramustine, irofulven, and pipobroman, are susceptible to overexpression. They affect the various systems after taking his amount greater than his recommended minimum levels. (Table 3).

Table 3: Toxicity analysis of selected alkylating agents

Classification	Target	Melphalan		Mitomycin C		Estramustine		Irofulven		Pipobroman	
		Prediction	Probability	Prediction	Probability	Prediction	Probability	Prediction	Probability	Prediction	Probability
Organ Toxicity	Hepatotoxicity	Inactive	0.88	Inactive	0.88	Active	0.65	Inactive	0.74	Inactive	0.97
	Neurotoxicity	Active	0.87	Active	0.53	Inactive	0.82	Inactive	0.85	Active	0.61
	Nephrotoxicity	Active	0.53	Active	0.83	Inactive	0.59	Inactive	0.75	Inactive	0.79
	Respiratory toxicity	Active	0.96	Active	0.93	Active	0.93	Active	0.86	Inactive	0.51
	Cardiotoxicity	Active	0.63	Inactive	0.73	Inactive	0.6	Inactive	0.56	Inactive	0.68
Toxicity Endpoints	Carcinogenicity	Active	0.8	Active	0.78	Inactive	0.53	Inactive	0.55	Inactive	0.65
	Immunotoxicity	Inactive	0.99	Inactive	0.61	Active	0.99	Inactive	0.67	Inactive	0.99
	Mutagenicity	Active	0.86	Active	0.81	Inactive	0.7	Active	0.69	Active	0.76
	Cytotoxicity	Inactive	0.64	Active	0.95	Inactive	0.54	Inactive	0.71	Inactive	0.81
	BBB-barrier	Active	0.58	Inactive	0.96	Active	0.8	Active	0.68	Active	0.99
	Ecotoxicity	Inactive	0.51	Inactive	0.63	Active	0.56	Inactive	0.57	Inactive	0.53
	Clinical toxicity	Active	0.59	Active	0.87	Active	0.66	Active	0.52	Active	0.7
	Nutritional toxicity	Active	0.8	Active	0.87	Active	0.51	Active	0.58	Active	0.51
Nuclear Receptor Signaling Pathways	AhR	Inactive	0.96	Inactive	0.98	Inactive	0.94	Inactive	0.9	Inactive	0.98
	Androgen R	Inactive	0.99	Inactive	0.98	Active	0.51	Inactive	0.86	Inactive	0.96
	AR-LBD	Inactive	0.99	Inactive	0.98	Inactive	0.94	Inactive	0.81	Inactive	0.96
	Aromatase	Inactive	0.98	Inactive	0.92	Inactive	0.92	Inactive	0.88	Inactive	0.99
	Estrogen R	Inactive	0.98	Inactive	0.9	Active	0.57	Inactive	0.78	Inactive	0.94
	ER-LBD	Inactive	0.99	Inactive	0.99	Inactive	0.63	Inactive	0.94	Inactive	0.99
	PPAR-Gamma	Inactive	0.98	Inactive	0.95	Inactive	0.96	Inactive	0.97	Inactive	0.99
Stress Response Pathways	nrf2/ARE	Inactive	0.99	Inactive	0.94	Inactive	0.97	Inactive	0.85	Inactive	0.99
	HSE	Inactive	0.99	Inactive	0.94	Inactive	0.97	Inactive	0.85	Inactive	0.99
	MMP	Inactive	0.92	Inactive	0.93	Inactive	0.84	Inactive	0.77	Inactive	0.96
	p53	Active	1	Active	1	Inactive	0.58	Inactive	0.9	Inactive	0.93
	ATAD5	Inactive	0.95	Inactive	0.98	Inactive	0.98	Inactive	0.97	Inactive	0.96
Molecular Initiating Events	THRÎ±	Inactive	0.81	Inactive	0.84	Active	0.71	Inactive	0.74	Inactive	0.76
	THRÎ²	Inactive	0.86	Inactive	0.88	Inactive	0.65	Inactive	0.93	Inactive	0.69
	Transtyretrin	Inactive	0.86	Inactive	0.76	Inactive	0.91	Active	0.59	Inactive	0.95
	Ryanodine R	Inactive	0.88	Inactive	0.87	Inactive	0.81	Inactive	0.9	Inactive	0.82
	GABA receptor	Inactive	0.68	Inactive	0.73	Inactive	0.52	Active	0.53	Inactive	0.64
	NMDAR	Inactive	0.61	Inactive	0.96	Inactive	0.96	Inactive	0.99	Inactive	0.85
	AMPAR	Inactive	0.99	Inactive	0.98	Inactive	1	Inactive	1	Inactive	0.99
	Kainate R	Inactive	1	Inactive	0.99	Inactive	1	Inactive	1	Inactive	1
	Ach E	Inactive	0.56	Inactive	0.58	Inactive	0.59	Inactive	0.73	Inactive	0.55
	CAR	Inactive	1	Inactive	0.95	Inactive	0.96	Inactive	0.99	Inactive	0.99
	PXR	Inactive	0.73	Active	0.52	Inactive	0.56	Active	0.57	Inactive	0.62
	NADHOX	Inactive	0.95	Inactive	0.86	Inactive	0.9	Inactive	0.58	Inactive	0.88
	VGSC	Inactive	0.62	Inactive	0.7	Inactive	0.83	Inactive	0.92	Inactive	0.65
	Na+/I- symporter	Inactive	0.9	Active	0.55	Inactive	0.97	Inactive	0.8	Inactive	0.93
Metabolism	CYP1A2	Inactive	0.92	Inactive	0.94	Inactive	0.91	Inactive	0.92	Inactive	0.97
	CYP2C19	Inactive	0.88	Inactive	0.82	Inactive	0.75	Inactive	0.82	Inactive	0.76
	CYP2C9	Inactive	0.84	Inactive	0.62	Inactive	0.51	Inactive	0.51	Inactive	0.72
	CYP2D6	Active	0.59	Inactive	0.72	Active	0.71	Inactive	0.81	Active	0.52
	CYP3A4	Active	0.95	Inactive	0.63	Inactive	0.77	Inactive	0.83	Inactive	0.92
	CYP2E1	Inactive	0.99	Inactive	0.98	Inactive	0.99	Inactive	0.99	Inactive	0.98

ADME properties of alkylating agents

The ADME properties showed that melphalan, mitomycin C, irofulven, and pipobroman are quite soluble and exhibit lower lipophilicity than estramustine. Pharmacokinetic findings showed that melphalan, irofulven, estramustine, and pipobroman are highly absorbed via the gastrointestinal tract, while mitomycin C is not (Table 4).

Table 4: ADME properties of selected alkylating agents

Properties	Physicochemical				
	Melphalan	Mitomycin	Irofulven	Estramustine	Pipobroman
Formula	$C_{13}H_{18}Cl_2N_2O_2$	$C_{15}H_{18}N_4O_5$	$C_{15}H_{18}O_3$	$C_{23}H_{31}Cl_2NO_3$	$C_{10}H_{16}Br_2N_2O_2$
Molecular weight	305.20 g/mol	334.33 g/mol	246.30g/mol	440.40 g/mol	356.05 g/mol
No. of heavy atoms	19	24	18	29	16

H. bond donors	2	3	2	1	0
H. bond acceptors	3	6	3	1	2
Molar refractivity	78.91	86.95	68.76	117.80	77.83
Lipophilicity					
Log p o/w (WLOGP)	1.92	-2.41	1.60	5.18	0.47
Water Solubility					
Class	Very soluble	Very soluble	Very soluble	Poorly soluble	Very soluble
Log S (SILICOS-IT)	-4.04	-1.19	-2.91	-6.08	-2.84
Pharmacokinetics					
GI absorption	High	Low	High	High	High
BBB permeant	Yes	No	Yes	Yes	Yes
Log Kp (skin permeation)	-8.02 cm/s	-8.62 cm/s	-7.94 cm/s	-6.15cm/s	-8.17 cm/s
Drug likeness					
Lipinski	Yes; 0 violation	Yes; 0 violation	Yes; 0 violation	Yes; 1 violation	Yes; 0
Bioavailability score	0.55	0.55	0.55	0.55	0.55

Possible mode of Action of alkylating agents against hepatocellular carcinoma

Estramustine

The molecular docking, ADME properties, and pharmacokinetic studies reveal that the best alkylating agent after the findings is estramustine, which typically inhibits the action of epidermal growth and fibroblast growth factors. Overexpression of both factors leads to the stimulation of PI3K/AKT/mTOR and MAPK/ERK pathways, which are involved in promoting proliferation and angiogenesis. Estramustine interferes with the cascade through Inhibition of EGFR phosphorylation, suppression of EGFR expression, inhibition of EGFR-mediated signaling, FGFR dimerization and phosphorylation, and FGF ligand expression. They decreased cell survival, migration, and proliferation, inhibited angiogenic signals and tumor vascularization, depriving the tumor of nutrients. So, estramustine causes Cell cycle arrest at G2/M, induces apoptosis, and suppresses EGF- and FGF-mediated oncogenic signaling (Fig. 5).

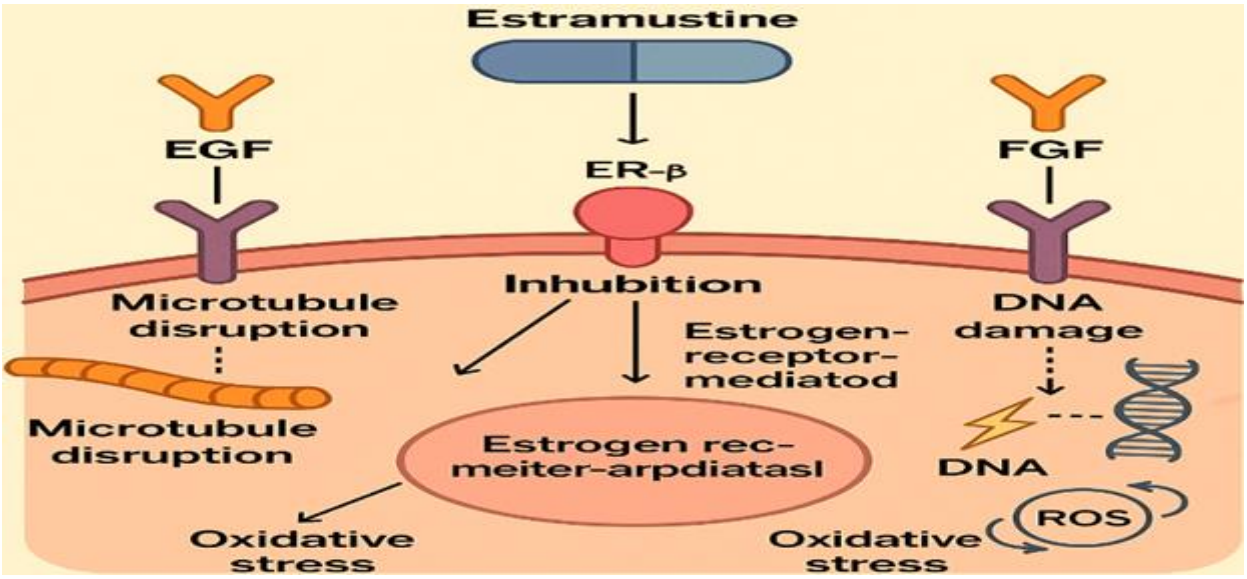

Fig. 5: Possible Mechanism of action of estramustine against HCC

Mitomycin C

Similarly, the second alkylating agent, which strongly inhibits the epidermal growth factor, is mitomycin C. Mitomycin C downregulates EGFR expression at the cell surface, inhibits phosphorylation (activation) of EGFR, prevents downstream PI3K/AKT and MAPK/ERK signaling pathways, thereby inhibiting: tumor cell proliferation, invasion, angiogenesis, and metastasis. Mitomycin C is activated in conditions of hypoxia (frequent in solid tumors); it creates DNA interstrand crosslinks at guanine bases. This inhibits DNA replication and transcription, resulting in Cell cycle arrest (G2/M phase) and apoptosis (Fig. 6).

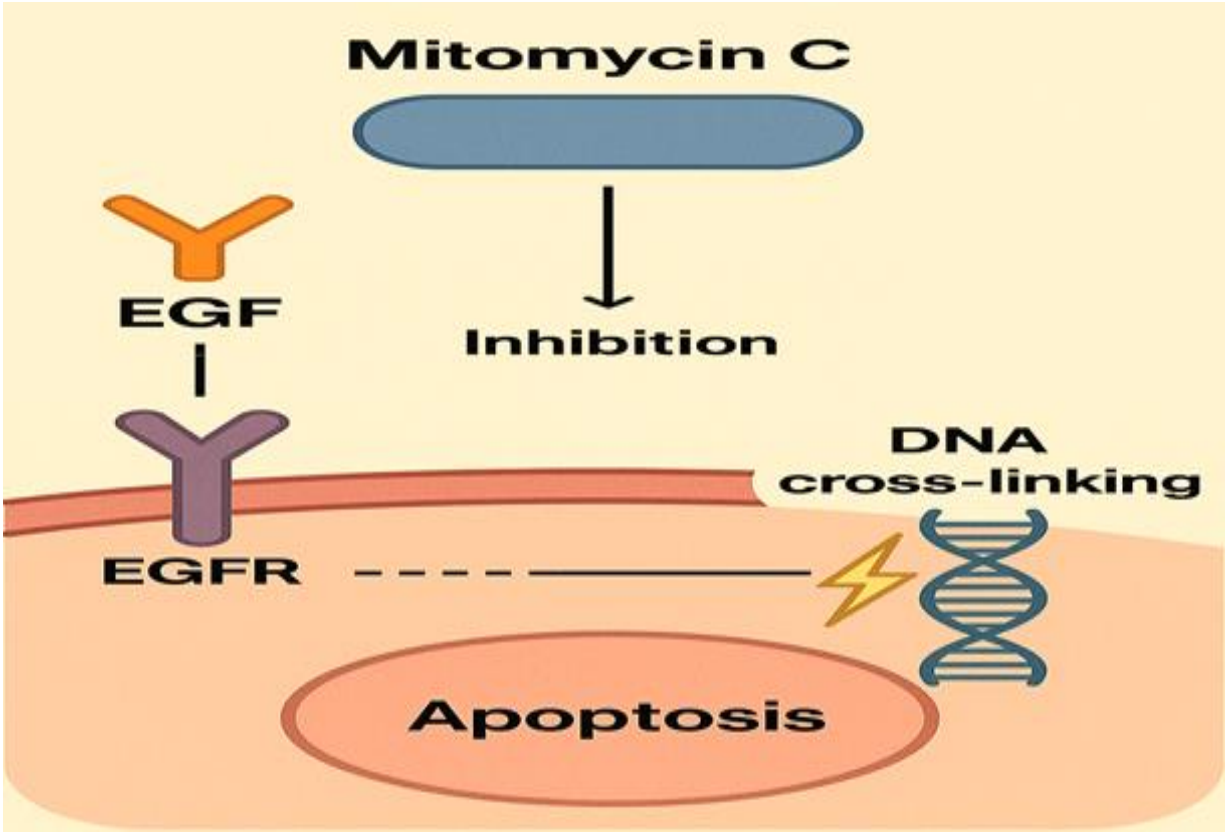

Fig. 6: Possible Mechanism of Action of Mitomycin in HCC

Irofulven

Like estramustine and mitomycin, Irofulven intercalates DNA and produces covalent adducts (alkylation), initiates transcriptional blockade and replication fork destruction, causes DNA double-strand breaks, G2/M phase arrest, Apoptosis, Blocks RNA Polymerase II, and Suppresses FGF-induced gene transcription (e.g., cyclins, VEGF). The activity is accountable for Reduced cell proliferation, Impaired angiogenesis, and Inhibition of tumor-promoting genes downstream of FGFR (Fig. 7).

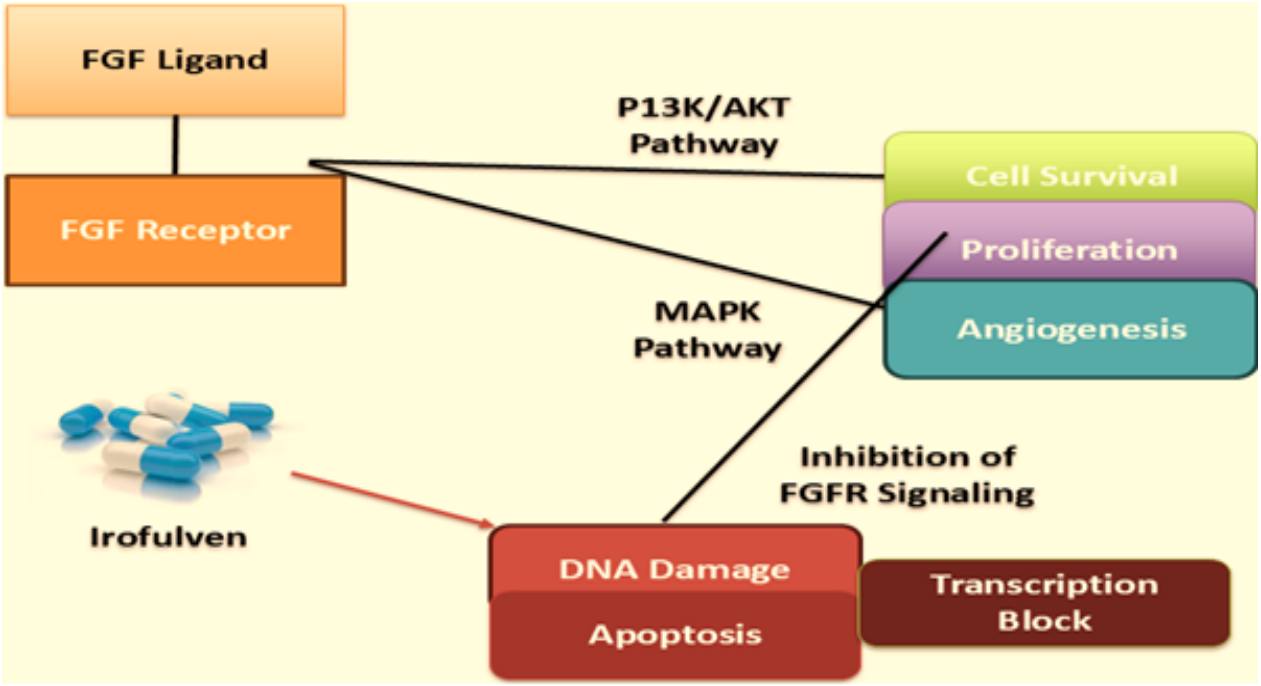

Fig. 7: Possible Mechanism of Action of Irofulven in HCC

Conclusion

The computational approach reflects that the selected five alkylating agents commonly inhibit the overexpression of the selected two target proteins that are involved in the progression of uncontrolled apoptosis and signaling pathways, leading to carcinogenesis. The most active alkylating agent was estramustine, which efficiently inhibits both targeting proteins. Along with estramustine, irofulven, melphalan, and mitomycin C also cause the inhibition of the proteins. The in silico molecular docking simulation showed that the target-specific alkylating agents might be used against other types of cancer, especially against hepatocellular carcinoma and hepatoblastoma in early age children. The findings suggested that targeted specific therapies may be significant against hepatocellular carcinoma in children as well as in adults, with appropriate concentration. Therefore, it is suggested that to confirm the in silico approaches, in vitro as well as in vivo trials should be performed and promote the use of different anticancer drugs against cancerous cells to stop carcinogenesis in humans.

References

Akhtar MT, Qadir R, Altaf U, Almas T, Batool S, Ikram MS, Meor Hussin AS, Perveen K, Alshaikh NA and Saadia M (2025). Phytochemical profiling and biological activities of Nigella sativa vinegar extract: an insight into hypoglycemic potential using in vivo and in silico studies. Chem Biodivers., **22(5)**: e202402512.

Anafcheh M, Ghafouri R and Naderi F (2012). Exploring electronic structures for the most stable isomers of C12B6N6 and B6N6C12 heterofullerenes based on NMR, NICS and NBO analysis: A DFT study. Physica E: Low-Dim Syst Nanostruct., **44(10)**: 1992–1998.

Arafeh R, Shibue T, Dempster JM, Hahn WC and Vazquez F (2025). The present and future of the Cancer Dependency Map. Nat Rev Cancer., **25(1)**: 59–73.

Bray F, Laversanne M, Sung H, Ferlay J, Siegel RL and Soerjomataram I (2024). Global cancer statistics 2022: GLOBOCAN estimates of incidence and mortality worldwide for 36 cancers in 185 countries. CA Cancer J Clin., **74(3)**: 229–263.

Cadoret A, Ovejero C, Saadi-Kheddouci S, Souil E, Fabre M, Romagnolo B, Kahn A and Perret C (2001). Hepatomegaly in transgenic mice expressing an oncogenic form of β-catenin. Cancer Res., **61(8)**: 3245–3249.

Collaborators GBDCRF (2020). The global burden of cancer attributable to risk factors, 2010–19: a systematic analysis for the Global Burden of Disease Study 2019. Lancet., **400(10352)**: 563–591.

Created in BioRender (2024). https://www.biorender.com

Diao X, Guo C, Jin Y, Li B, Gao X, Du X and Qiu H (2025). Cancer situation in China: an analysis based on the global epidemiological data released in 2024. Cancer Commun., **45(2)**: 178–197.

Diseases GBD and Injuries C (2024). Global incidence, prevalence, years lived with disability (YLDs), disability-adjusted life-years (DALYs), and healthy life expectancy (HALE) for 371 diseases and injuries in 204 countries and territories and 811 subnational locations, 1990-2021: a systematic analysis for the Global Burden of Disease Study 2021. Lancet., 403(10440): 2133-2161.

Filho AM, Laversanne M, Ferlay J, Colombet M, Piñeros M, Znaor A and Bray F (2025). The GLOBOCAN 2022 cancer estimates: data sources, methods, and a snapshot of the cancer burden worldwide. Int J Cancer., **156(7)**: 1336–1346.

Han-You X (2013). Chronic infection and other risk factors of cancer in China and other countries. Ann Oncol., **24(1)**: 267.

Kim M, Lee HC, Tsedensodnom O, Hartley R, Lim YS, Yu E, Merle P and Wands JR (2008). Functional interaction between Wnt3 and Frizzled-7 leads to activation of the Wnt/β-catenin signaling pathway in hepatocellular carcinoma cells. J Hepatol., **48(5)**: 780–791.

Laurent–Puig P, Legoix P, Bluteau O, Belghiti J, Franco D, Binot F, Monges G, Thomas G, Bioulac–Sage P and Zucman–Rossi J (2001). Genetic alterations associated with hepatocellular carcinomas define distinct pathways of hepatocarcinogenesis. Gastroenterology., **120(7)**: 1763–1773.

McCubrey JA, Abrams SL, Fitzgerald TL, Cocco L, Martelli AM, Montalto G, Cervello M, Scalisi A, Candido S, Libra M and Steelman LS (2015). Roles of signaling pathways in drug resistance, cancer initiating cells and cancer progression and metastasis. Adv Biol Regul., **57**: 75–101.

Nejak-Bowen KN, Thompson MD, Singh S, Bowen WC Jr, Dar MJ, Khillan J, Dai C and Monga SP (2010). Accelerated liver regeneration and hepatocarcinogenesis in mice overexpressing serine-45 mutant β-catenin. Hepatology., **51(5)**: 1603–1613.

Paz MM, Zhang X, Lu J and Holmgren A (2012). A new mechanism of action for the anticancer drug mitomycin C: mechanism-based inhibition of thioredoxin reductase. Chem Res Toxicol., **25(7)**: 1502–1511.

Pocasap P, Nonpunya A and Weerapreeyakul N (2021). Pinus kesiya Royle ex Gordon induces apoptotic cell death in hepatocellular carcinoma HepG2 cell via intrinsic pathway by PARP and Topoisomerase I suppression. Biomed Pharmacother., **139**: 111628.

ProTox-3.0 (2024). Prediction of toxicity of chemicals. https://tox-new.charite.de/protox_III.

Quintanal-Villalonga Á, Chan JM, Yu HA, Pe'er D, Sawyers CL, Sen T and Rudin CM (2020). Lineage plasticity in cancer: a shared pathway of therapeutic resistance. Nat Rev Clin Oncol., **17(6)**: 360–371.

Rebouissou S, Franconi A, Calderaro J, Letouzé E, Imbeaud S, Pilati C, Nault JC, Couchy G, Laurent A, Balabaud C and Bioulac-Sage P (2016). Genotype-phenotype correlation of CTNNB1 mutations reveals different β-

catenin activity associated with liver tumor progression. Hepatology., **64(6)**: 2047–2061.

Rubin E, Shan KS, Dalal S, Vu DU, Milillo-Naraine AM, Guaqueta D and Ergle A (2024). Molecular targeting of the human epidermal growth factor receptor-2 (HER2) genes across various cancers. Int J Mol Sci., **25(2)**: 1064.

Santos AA, Delgado TC, Marques V, Ramirez-Moncayo C, Alonso C, Vidal-Puig A, Hall Z, Martínez-Chantar ML and Rodrigues CM (2024). Spatial metabolomics and its application in the liver. Hepatology., **79(5)**: 1158–1179.

Schulze RJ, Schott MB, Casey CA, Tuma PL and McNiven MA (2019). The cell biology of the hepatocyte: a membrane trafficking machine. J Cell Biol., **218(7)**: 2096–2112.

Shi JH, Guo WZ, Jin Y, Zhang HP, Pang C, Li J, Line PD and Zhang SJ (2019). Recognition of HER2 expression in hepatocellular carcinoma and its significance in postoperative tumor recurrence. Cancer Med., **8(3)**: 1269–1278.

Singh SP, Madke T and Chand P (2025). Global epidemiology of hepatocellular carcinoma. J Clin Exp Hepatol., **15(2)**: 102446.

Sun Y, Wu P, Zhang Z, Wang Z, Zhou K, Song M, Ji Y, Zang F, Lou L, Rao K and Wang P (2024). Integrated multi-omics profiling to dissect the spatiotemporal evolution of metastatic hepatocellular carcinoma. Cancer Cell., **42(1)**: 135–156.

SwissADME (2024). ADME parameter prediction tool. https://www.swissadme.ch/

Welch DR and Hurst DR (2019). Defining the hallmarks of metastasis. Cancer Res., **79**: 3011–3027.

World Health Organization. Global Health Observatory. Geneva. Accessed: June 2024. http://www.who.int/data/gho

Yip HY and Papa A (2021). Signaling pathways in cancer: therapeutic targets, combinatorial treatments, and new developments. Cells., **10(3)**: 659.